



Case Report

MRI-PET fusion biopsy in prostate cancer at Lerdsin Hospital: two cases report

Varathorn Lumyai^{1,2}

¹Department of Urology, Lerdsin Hospital, Ministry of Health, ²Rungsit University, Bangkok, Thailand

Keywords:

Prostate cancer,
MRI-PET fusion,
targeted biopsy,
mpMRI, PSMA PET,
image-guided biopsy

Abstract

MRI-PET fusion biopsy is a novel technique that enhances the accuracy of prostate lesion localization and sampling. This method potentially improves diagnostic precision when compared with conventional MRI-guided biopsy. In the two cases described here MRI-PET fusion ultrasound biopsy was utilized for prostate cancer evaluation. A 65-year-old male with a prostate-specific antigen (PSA) level of 8.0 ng/ml underwent prostate MRI, which revealed two suspicious lesions (PI-RADS 5 and PI-RADS 4). MRI-PET imaging alone identified only the PI-RADS 5 lesion (SUVmax 21.51) and an additional area of uptake in the transitional zone (SUV 6.83). Fusion biopsy confirmed adenocarcinoma Gleason score (GS) 4 + 4 and 4 + 3 in the PI-RADS 5 and 4 lesions, respectively, while the transitional zone was benign (BPH). Laparoscopic radical prostatectomy confirmed GS 4 + 4 with 10% tumor involvement. The second case involved a 75-year-old male with a PSA level of 7.53 ng/ml who underwent MRI, which demonstrated PI-RADS 5 and 3 lesions. PET imaging showed positive uptake in both (SUVmax 10.53). Fusion biopsy revealed benign prostatic hyperplasia in both lesions. In these two cases, MRI-PET fusion ultrasound biopsy enabled improved lesion detection and boundary delineation in comparison with standard MRI. Although slightly more expensive, this technique may enhance diagnostic accuracy. Further studies are warranted to evaluate its role in patients with PSA levels of 4–10 ng/ml.

Insight Urol 2025;46(2):130-6. doi: 10.52786/isu.a.113

Introduction

MRI-PET fusion prostate biopsy for prostate cancer detection

Prostate cancer is one of the most prevalent malignancies affecting men worldwide. Its early and accurate detection is crucial for effective treatment and improved outcomes. Traditional diagnostic methods, including prostate-specific

antigen (PSA) testing and digital rectal examination (DRE), have limited specificity and sensitivity, often resulting in unnecessary biopsies or missed diagnoses.¹ Standard transrectal ultrasound (TRUS)-guided biopsy, although commonly used, also lacks precision in targeting suspicious intra-prostatic lesions.²

Corresponding author: Varathorn Lumyai

Address: Department of Urology, Lerdsin Hospital, Ministry of Health, Rungsit University, Bangkok 10500, Thailand

E-mail: lumyai2509@gmail.com

Manuscript received: May 29, 2025

Revision received: October 28, 2025

Accepted after revision: November 21, 2025



Multiparametric magnetic resonance imaging (mpMRI) has substantially enhanced the detection and localization of clinically significant prostate cancer (csPCA) by providing high-resolution anatomical and functional information.³ Prostate-specific membrane antigen (PSMA) is a 750-amino acid type II membrane glycoprotein highly expressed in prostate cancer cells but present at low levels in normal prostate and certain non-prostatic tissues (e.g., kidneys and salivary glands). It plays a critical role in both diagnostic imaging and therapeutic targeting of prostate cancer. Radiotracers such as ⁶⁸Ga-PSMA-11 or ¹⁸F-DCFPyL, enable highly sensitive detection of prostate cancer lesions at primary, metastatic, or recurrent sites, outperforming conventional imaging modalities (CT, MRI, bone scan), particularly in cases with low PSA levels.^{4,5}

MRI-PET fusion prostate biopsy involves the co-registration of mpMRI and PET images to generate a detailed map of the prostate, identifying areas of increased metabolic activity suggestive of malignancy. These fused images guide targeted biopsies, improving sampling accuracy while minimizing unnecessary tissue extraction.⁶ Studies have demonstrated that MRI-PET fusion biopsy increases the detection rate of clinically significant prostate cancer in comparison to conventional TRUS-guided biopsy, especially in patients with prior negative biopsy results but persistently elevated PSA levels.⁷

A recent study confirmed similar findings, particularly among patients at high risk of prostate cancer, showing a diagnostic accuracy of ⁶⁸Ga-PSMA PET/CT at 92.0% compared with 86.2% for mpMRI.⁸

The PRIMARY score is a five-category scale developed to identify csPCA on ⁶⁸Ga-PSMA-11 PET/CT using a combination of anatomical sites, uptake pattern, and intensity. Previous studies reported an area under the curve (AUC) of 0.796 (95% confidence interval (95%CI): 0.738-0.853) for the PRIMARY score and 0.851 (95%CI: 0.783-0.918) for SUV_{max}, although the specificity of the PRIMARY score was limited to 65.0% when comparing scores 3-5 versus 1-2.⁹

By integrating the superior anatomical resolution of an MRI with the metabolic and molecular imaging capabilities of a PET, MRI-PET fusion biopsy represents a significant advancement in prostate cancer diagnostics. It offers several potential advantages including reduced detection of

indolent tumors, improved risk stratification, and enhanced guidance for focal therapy and active surveillance.¹⁰ The aim of this study is to apply the technique in two patients with PSA levels between 4-10 ng/ml to evaluate the procedural steps, advantages, and limitations of this newly introduced method in Thailand.

Case Report

Case 1

A 65-year-old Thai male with a history of dyslipidemia and previous transitional cell carcinoma (TCC) of the right renal pelvis presented with lower urinary tract symptoms (LUTS) and an elevated PSA level of 8.0 ng/ml. He had undergone laparoscopic right nephroureterectomy with bladder cuff excision three years earlier. To further evaluate his condition, mpMRI combined with ¹⁸F-PSMA PET was performed at Chulabhorn Hospital.

Imaging findings:

- MRI findings:

- o A lesion measuring $0.9 \times 0.6 \times 0.9$ cm with marked diffusion restriction located in the right anterior transition zone, classified as PI-RADS 5 (lesion A).

- o A second lesion, measuring 0.5 cm, located in the right peripheral zone, corresponding to PI-RADS 4 (lesion B).

- ¹⁸F-PSMA PET/MRI findings:

- o A PSMA-avid hypo-T2 nodule ($0.9 \times 0.6 \times 0.9$ cm) with significant diffusion restriction in the right anterior transition zone at the mid-gland level (SUV = 21.51), suspicious for malignancy (lesion C).

- o Diffuse mild PSMA uptake (standardized uptake value (SUV) = 6.83) in a symmetrical hypo-T2 lesion with moderate diffusion restriction at the posterior paramedian region of the prostatic base (lesion D).

The patient received a rectal enema the day before the procedure and an intravenous dose of ceftriaxone 2 gm administered 30 minutes prior to surgery. Before biopsy, ¹⁸F-PSMA PET/MRI data were imported into the Koelis Trinity System (Model KURO-3000) workstation, and prostate boundaries were delineated on MRI. A SUV threshold of 2.5 was used to define PET-positive lesions¹¹, which were marked as biopsy targets. Lesion SUV and volume were recorded for analysis.



Under spinal anesthesia and with Trendelenburg positioning, the MRI-defined prostate volume (from T2W images) was registered with the real-time 3D transrectal ultrasound data using the Koelis system's tracking algorithm, allowing precise localization of PET-positive targets for biopsy. Transperineal biopsies were then performed and divided into five groups according to imaging correlation and sampling strategy:

- Group 1: MRI (+), PET (+) — Lesion A = Lesion C (SUV = 21.51)
- Group 2: MRI (+), PET (-) — Lesion B
- Group 3: MRI (-), PET (+) — Lesion D (SUV = 6.83)
- Group 4: Systematic (random) biopsy – right peripheral zone
- Group 5: Systematic (random) biopsy – left peripheral zone

Collected tissue samples were sent to the Institute of Pathology, Ministry of Public Health. After the biopsy, the patient was admitted for observation for 24-hours and discharged the following day. He was prescribed ciprofloxacin 500 mg twice daily for five days and advised to return immediately if complications occurred. Post-procedure, he experienced mild hematuria for two days with no other adverse events. Follow-up for pathology results was scheduled for two weeks post-op (Fig. 1).

Pathological results

- Group 1: Prostatic acinar adenocarcinoma, Gleason score 4+4 = 8 (Grade Group 4)
 - Tumor involved 2 of 7 cores (~5% of total tissue)
 - Cribiform glands: present
 - Perineural invasion: not identified
- Group 2: Prostatic acinar adenocarcinoma, Gleason score 4+3 = 7 (Grade Group 3)
 - Tumor involved 1 of 6 cores (~20% of total tissue)
 - Cribiform glands: present
 - Perineural invasion: not identified
- Group 3: Benign prostatic tissue
- Group 4: Prostatic acinar adenocarcinoma, Gleason score 3+3 = 6 (Grade Group 1)
 - Tumor involved 1 of 6 cores (~2% of total tissue)
 - Cribiform glands: not identified
 - Perineural invasion: not identified
- Group 5: Benign prostatic tissue

3 months later, the patient underwent a laparoscopic radical prostatectomy with bilateral pelvic lymph node dissection. Intraoperatively, mild adhesion was noted at the perineum, with an estimated blood loss of 100 ml. The pathological report revealed the following findings:

Prostate gland

- Diagnosis: acinar adenocarcinoma
- Gleason Score: 4 + 4 = 8 (Grade Group 4)
- Intraductal carcinoma: present
- Tumor involvement: approximately 10% of the entire prostate gland
- Cribiform glands: present
- Extraprostatic extension: not identified
- Seminal vesicle invasion: not identified
- Surgical margins: all resection margins free of tumor
- Lymphovascular invasion: not identified
- Perineural invasion: not identified

Pelvic lymph nodes

- Metastasis: No evidence of metastatic disease in examined lymph nodes

Case 2

A 75-year-old Thai male with a medical history of psoriasis presented with a six-month history of lowLUTS, including urinary frequency, urgency, nocturia (2–3 times per night), and a sensation of incomplete bladder emptying. He had no history of urinary tract infections, hematuria, or urinary retention. Initial treatment with alfuzosin (Xatral XL) 10 mg once daily at bedtime resulted in partial improvement of symptoms. The PSA level at presentation was 4.37 ng/ml, however, a repeat test three months later revealed a rise to 7.53 ng/ml, prompting further evaluation with multiparametric MRI (mpMRI).

MRI findings:

- A 2.4×1.6 cm lesion in the left transitional zone extending from the base to the mid-gland and involving the peripheral zone. The lesion exhibited capsular bulging, raising suspicion for extraprostatic extension, and was classified as PI-RADS 5 (version 2.1).
- A 1.0 cm low-T2-signal nodule with an indistinct margin in the right transitional zone at the mid-gland level, classified as PI-RADS 3 (version 2.1).



Figure 1. MRI-PET fusion prostate biopsy in case 1

- No evidence of suspicious pelvic lymphadenopathy.

PSMA PET-MRI findings

- A PSMA-avid lesion on the left side at the mid-apex, measuring $2.3 \times 1.8 \times 1.2$ cm, with a maximum standardized uptake value (SUVmax) of 10.52, corresponding to the PI-RADS 5 lesion.
- A second PSMA-avid lesion in the right

mid-gland transitional zone, measuring $1.3 \times 1.1 \times 1.2$ cm, with an SUVmax of 10.53, corresponding to a PI-RADS 4 lesion.

An MRI/PSMA-PET/ultrasound fusion-guided biopsy was subsequently performed. Targeted biopsies were obtained from both the left transitional zone and the right mid-gland lesions, along with systematic biopsies from the right and left prostate lobes (Fig. 2).

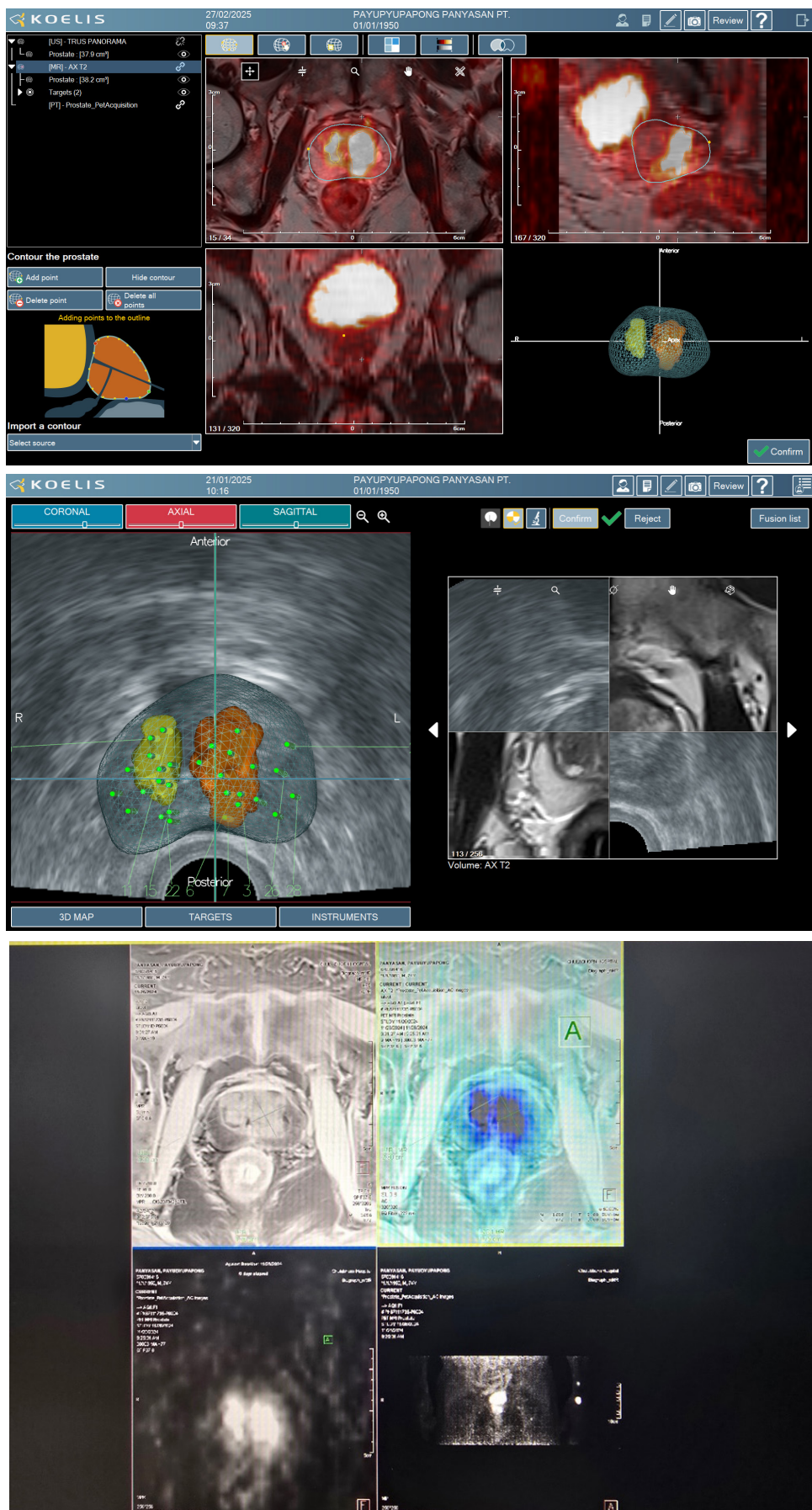


Figure 2. MRI–PET fusion prostate biopsy in case 2



Post-procedure, the patient experienced mild hematuria for one day without other adverse events. Pathological examination revealed that all sampled cores, including both targeted and systematic biopsies, showed benign prostatic hyperplasia (BPH) with no evidence of malignancy.

Discussion

MRI of the prostate is now widely used to identify suspicious lesions before biopsy. Recent systematic reviews and meta-analyses evaluating PI-RADS v2.1 reported approximate detection rates of clinically significant prostate cancer (csPCa) as 12%, 60%, and 85% for PI-RADS 3, 4, and 5 lesions, respectively. These results confirm that higher PI-RADS scores show a strong correlation with an increased likelihood of detecting csPCa.^{12,13} MRI-ultrasound fusion prostate biopsy provides high soft-tissue resolution, particularly for lesions located in the peripheral zone. Recent meta-analyses have demonstrated a sensitivity of 87-93% and a specificity of 68-75%.^{14,15}

mpMRI and prostate-specific membrane antigen positron emission tomography (PSMA-PET) have become critical tools in the diagnosis and management of csPCa. PSMA-PET. This is particularly evident when combined with MRI (PSMA PET/MRI), which further improves diagnostic performance, with a reported sensitivity of 97% and specificity of 66%. The pooled negative likelihood ratio (NLR) for PSMA PET/CT is 0.05, a score superior to the 0.16-0.26 reported for mpMRI.^{16,17} Yujia Li et al. reported an area under the receiver operating characteristic curve (AUC) for the PRIMARY score, SUVmax, and PSMA-PET to be 0.796 (95%CI: 0.738-0.853), 0.851 (95%CI: 0.783-0.918), and 0.806 (95% CI: 0.742-0.870), respectively, with an SUVmax cutoff value of 6.5 corresponding to a specificity of 79%.¹¹

This study supports the premise that the PI-RADS scoring system depends heavily on radiological expertise. Emerging techniques such as PSMA PET/MRI may improve lesion localization and help refine patient selection, potentially reducing unnecessary biopsies. To date most urologists are less familiar with the interpretation of PI-RADS than radiologists, PET/MRI may enhance lesion identification and diagnostic confidence, especially among younger or less experienced clinicians.

In our experience, the procedural workflow of PSMA-PET fusion biopsy closely resembles that of MRI-ultrasound fusion biopsy. However, PSMA-PET fusion provides clearer lesion boundaries due to distinct tracer uptake, allowing for more accurate targeting. This advantage reduces reliance on advanced radiological interpretation. However, despite this benefit, the cost of PSMA PET/MRI remains higher, at approximately 5,000 THB at Chulabhorn Hospital, posing a limitation for routine use. Furthermore, PSMA uptake may occur in benign conditions such as adenoma or prostatitis; therefore, SUVmax values must be interpreted cautiously when determining biopsy indications.

In case 1, MRI demonstrated a lesion in the right anterior transitional zone (PI-RADS 5) and another in the right peripheral zone (PI-RADS 4). PSMA-PET imaging showed uptake only in the first lesion, possibly due to the small size (5 mm) or a false-negative result in the second. The lesion with high SUVmax (21.51) corresponded to adenocarcinoma with a Gleason score of 4 + 4 (Grade group 4), consistent with prior evidence indicating that an SUVmax ≥ 8 is strongly associated with csPCa.¹⁰

In case 2, MRI revealed a larger lesion (2.4 \times 1.6 cm) classified as PI-RADS 5, with PSMA-PET showing concordant uptake (SUVmax 10.53). However, histopathology revealed benign prostatic hyperplasia. This discrepancy contrasts with previous findings¹⁰ and may suggest that the SUVmax cutoff predictive of csPCa could be higher in Asian populations compared to Western cohorts or reflect a potential false-positive PET result. This is based on a study of only two individuals but the findings warrant a more extensive study with a larger sample size.

Conclusion

These observations raise important considerations regarding optimal SUV thresholds for malignancy prediction. Limitations of our report include the novelty of the biopsy technique, variability in SUVmax measurement between institutions, and the higher cost compared with standard diagnostic methods, which may affect cost-effectiveness and accessibility. A potential focus for future research could involve the establishment of correlations between SUV values and Gleason scores, defining clinically meaningful



SUV cutoff values to distinguish prostate cancer from benign conditions. This would validate the diagnostic accuracy and cost-effectiveness of PSMA PET/MRI-guided biopsy in routine clinical practice, particularly among patients with PSA levels between 4-10 ng/ml.

References

1. Siegel RL, Miller KD, Fuchs HE, Jemal A. Cancer statistics, 2023. CA Cancer J Clin 2023;73:17-48.
2. Yamada Y, Ukimura O, Kaneko M, Matsugasumi T, Fujihara A, Vourganti S, et al. Moving away from systematic biopsies: image-guided prostate biopsy (in-bore biopsy, cognitive fusion biopsy, MRUS fusion biopsy)-literature review. World J Urol 2021;39:677-86.
3. Weinreb JC, Barentsz JO, Choyke PL, Cornud F, Haider MA, Macura KJ, et al. PI-RADS Prostate Imaging – Reporting and Data System: 2015, Version 2. Eur Urol 2016;69:16-40.
4. Afshar-Oromieh A, Avtzi E, Giesel FL, Holland-Letz T, Linhart HG, Eder M, et al. The diagnostic value of PET/CT imaging with the 68Ga-labelled PSMA ligand HBED-CC in the diagnosis of recurrent prostate cancer. Eur J Nucl Med Mol Imaging 2015;42:197-20.
5. Calais J, Czernin J, Cao M, Kishan AU, Hegde JV, Shaverdian N, et al. 68Ga-PSMA-11 PET/CT mapping of prostate cancer biochemical recurrence after radical prostatectomy in 270 patients with PSA <1.0 ng/mL: impact on salvage radiotherapy planning. J Nucl Med 2019;60:933-9.
6. Sonne I, Flker ER, Lenis AT, Sisk AE, Bahri S, Auerbach MA, et al. Head-to-Head Comparison of 68Ga-PSMA-11 PET/CT and mpMRI with a Histopathology Gold Standard in the Detection, Intraprostatic Localization, and Determination of Local Extension of Primary Prostate Cancer: Results from a Prospective Single-Center Imaging Trial. J Nucl Med 2022;63:847-54.
7. Wang R, Shen G, Yang R, Ma X, Tien R. 68Ga-PSMA PET/MRI for the diagnosis of primary and biochemically recurrent prostate cancer: A meta-analysis. Eur J Radiol 2020;130:109131.
8. Pepe P, Pennisi M. Targeted Biopsy in Men High Risk for Prostate Cancer: 68Ga-PSMA PET/CT Versus mpMRI. Clin Genitourin Cancer 2023;21:639-42.
9. Li Y, Li J, Yang J, Xiao L, Zhou M, Cai Y, et al. Using a novel PSMA-PET and PSA-based model to enhance the diagnostic accuracy for clinically significant prostate cancer and avoid unnecessary biopsy in men with PI-RADS ≤ 3 MRI. Eur J Nucl Med Mol Imaging 2025;52:913-24.
10. Rowe SP, Salavati A, Werner RA, Pienta KJ, Gorin MA, Pomper MG, et al. 18F-Labeled Radiotracers for Prostate-specific Membrane Antigen: Historical Perspective and Future Directions. PET Clin 2022;17:585-93.
11. Maurer T, Schnabel K, Schmidt F. Diagnostic performance of 68 Gallium-PSMA-11 PET/CT to detect primary prostate cancer. Oncotarget. 2017;8:104538-44.
12. Turkbey B, Rosenkrantz AB, Haider MA, Padhani AR, Villeirs G, Macura KJ, et al. Prostate Imaging Reporting and Data System version 2.1: 2019 update of Prostate Imaging Reporting and Data System version 2. Eur Urol 2019;76:340-51.
13. Girometti R, Giannarini G, De Martino M, Caregnato E, Cereser L, Soligo M, et al. Multivariable stratification of PI-RADS version 2.1 categories for the risk of false-positive target biopsy: Impact on prostate biopsy decisions. Eur J Radiol 2023;165:110897.
14. Ahmed HU, El-Shater Bosaily A, Brown LC, Gabe R, Kaplan R, Parmar MK, et al. Diagnostic accuracy of multi-parametric MRI and TRUS biopsy in prostate cancer (PROMIS): a paired validating confirmatory study. Lancet 2017;389:815-22.
15. Woo S, Suh CH, Kim SY, Cho JY, Kim SH, Moon MH. Head-to-Head Comparison Between Biparametric and Multiparametric MRI for the Diagnosis of Prostate Cancer: A Systematic Review and Meta-Analysis. AJR Am J Roentgenol 2018;211:W226-37.
16. Ling SW, de Jong AC, Schoots IG, Nasserinejad K, Busstra MB, et al. Comparison of 68Ga-labeled Prostate-specific Membrane Antigen Ligand Positron Emission Tomography/Magnetic Resonance Imaging and Positron Emission Tomography/Computed Tomography for Primary Staging of Prostate Cancer: A Systematic Review and Meta-analysis. Eur Urol Open Sci 2021;33:61-71.
17. Hope TA, Goodman JZ, Calais J, Behr SC, Hattangadi-Gluth JA, Barbuto DA, et al. Diagnostic accuracy of 68Ga-PSMA-11 PET for regional lymph node staging in high-risk prostate cancer: A prospective multicenter imaging trial. JAMA Oncol 2021;7:1635-42.